Interference in disordered systems: A particle in a complex random landscape

Alexander Dobrinevski, Pierre Le Doussal, and Kay Jörg Wiese

Interference in disordered systems: A particle in a complex random landscape

Alexander Dobrinevski,* Pierre Le Doussal,† and Kay Jörg Wiese‡

CNRS-Laboratoire de Physique Théorique de l'Ecole Normale Supérieure, 24 rue Lhomond, 75005 Paris Cedex-France

We consider a particle in one dimension submitted to amplitude and phase disorder. It can be mapped onto the complex Burgers equation, and provides a toy model for problems with interplay of interferences and disorder, such as the NSS model of hopping conductivity in disordered insulators and the Chalker-Coddington model for the (spin) quantum Hall effect. We also propose a direct realization in an experiment with cold atoms. The model has three distinct phases: (I) a *high-temperature* or weak disorder phase, (II) a *pinned* phase for strong amplitude disorder, and (III) a *diffusive* phase for strong phase disorder, but weak amplitude disorder. We compute analytically the renormalized disorder correlator, equivalent to the Burgers velocity-velocity correlator at long times. In phase III, it assumes a universal form. For strong phase disorder, interference leads to a logarithmic singularity, related to zeroes of the partition sum, or poles of the complex Burgers velocity field. These results are valuable in the search for the adequate field theory for higher-dimensional systems.

PACS numbers: 02.50.Ey, 05.40.Jc, 72.15.Rn

I.   INTRODUCTION

Much progress has been accomplished in the understanding of the thermodynamics of classical disordered systems [1, 2]. Typically, the disorder is modeled by a random potential. At low temperature, the low lying local minima of the resulting, rough, energy landscape become metastable states, and dominate the partition sum of the system. The correlations of the random potential determine the statistics of these metastable states, and hence the physics of the model. In many cases, for example in elastic disordered systems, the scaling of observables can be described by a family of $T = 0$ fixed points of the RG flow (most notably random-field and random-bond), which yield characteristic, universal roughness exponents and effective disorder correlators [3–5].

However, the picture is much less clear when quantum interference is important. In real time dynamics one must study a sum over Feynman paths, whose weights are complex random numbers. The dominant contributions may then be difficult to discern.

To give a specific example, hopping conductivity of electrons in disordered insulators in the strongly localized regime is described by the Nguyen-Spivak-Shklovskii (NSS) model [6]. The probability amplitude $J(a, b)$ is the sum over interfering directed paths Γ from a to b [7–11]

$$J(a, b) := \sum_{\Gamma} \prod_{j \in \Gamma} \eta_j \ . \tag{1}$$

The conductivity between sites a and b (e.g. on a $\mathbb{Z}^d$ lattice) is then given by $g(a, b) \sim |J(a, b)|^2$. Each lattice site j contributes a random sign $\eta_j = \pm 1$ (or, more generally a complex phase $\eta_j = e^{i\theta_j}$).

*dobrinev@lpt.ens.fr
†ledou@lpt.ens.fr
‡wiese@lpt.ens.fr

Another example is the Chalker-Coddington model [12] for the quantum Hall (and spin quantum Hall) effect, where the transmission matrix T, and the conductance $g(a, b) \sim \text{tr } T(a, b)^\dagger T(a, b)$, between two contacts a and b is given by [13, 14]:

$$T(a, b) = \sum_{\Gamma} \prod_{(ij) \in \Gamma} S_{(ij)} \ . \tag{2}$$

The random variables $S_{(ij)}$ on every bond (ij) are $U(N)$ matrices, with $N = 1$ for the charge quantum Hall effect and $N = 2$ for the spin quantum Hall effect. Here Γ are paths subject to some rules imposed at the vertices.

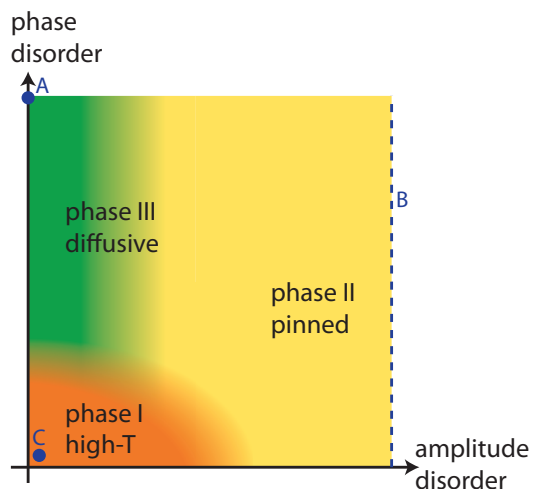In both models, one would like to understand the dom-

FIG. 1: (Color online) Phase portrait of the model. The horizontal axis is the strength of V and the vertical axis the strength of θ. The effective disorder correlators for points A (deep in the diffusive phase), B (deep in the pinned phase), C (infinitesimally small disorder) are analyzed in sections III, IV and V, respectively.

inating contributions to the sum over paths with random weights, given by $J(a, b)$ or $T(a, b)$, respectively; we shall denote it by Z in the following. In contrast to the thermodynamics of classical models, where all contributions are positive, contributions between paths with different phases can now cancel. One is also interested in the expected phase transitions, i.e. critical values for the amplitude and phase disorder above which interference effects become important.

This is a complicated problem. In this article, we therefore consider a toy model motivated by the models above, for which many computations can be done explicitly. More precisely, we analyze a "partition sum" Z defined in one dimension, of the form

$$Z(w) = \sqrt{\frac{\beta m^2}{2\pi}} \int_{-\infty}^{\infty} \mathrm{d}x\, e^{-\beta\left[V(x) + \frac{m^2}{2}(x-w)^2\right] - i\theta(x)} \quad (3)$$

Here, $V(x)$ is a random potential and $\theta(x)$ a random phase, both with translationally invariant correlations, and $\beta = 1/T$ the inverse temperature. This is a toy model defined in one dimension and thus a drastic simplification compared to both the NSS model (1) and the Chalker-Coddington model (2) (which are usually considered in two dimensions and above). However, a similar toy model for a random potential without random phases reproduces many important physical features of realistic, higher-dimensional models. For example, the appearance of shocks and depinning are already present in this framework [15–17]. For purely imaginary disorder, a nice experimental realization of the sum in (3) in cold atom physics is discussed in Section II B. Complex sums similar to (3) are also encountered in magnetization relaxation in random magnetic fields, see e.g. [18].

The interplay between random phases $\theta(x)$ and a random potential $V(x)$ similar to (3) was already studied, among others, in [19–22]. The basic distinction of three phases, high-temperature phase I, frozen phase II, and strong-interference phase III, was established by Derrida in [23], and we follow his conventions. The aim of this paper is to pursue a complementary approach to [23], based on the study of renormalized disorder correlation functions. The latter is defined due to the presence of the parabolic well centered at $x = w$ in (3). The resulting spatial structure exhibits non-trivial features such as, in some cases, discontinuous jumps (shocks) as w is varied. Furthermore the renormalized disorder correlator is the central object of the field theoretic treatment of disordered systems based on the functional renormalization group [16, 24], and thus the results of the toy model will give hints for a treatment of more realistic, higher-dimensional systems.

This article is organized as follows: In section II, we give the theoretical framework for our treatment. The model (3) is related to a complex Burgers equation, with time $t = m^{-2}$, which has generated interest in the mathematics community recently [25]. Equal-time correlation functions of the Burgers velocity field are the *renormalized disorder correlation functions* $\Delta(w - w')$ of our

model, $\overline{\partial_w \ln(Z(w)) \partial_{w'} \ln(Z(w'))}$. The precise definition is given in Sec. II D. They encode physical properties of the system like the appearance of shocks. Their $m \to 0$ (i.e. $t \to \infty$ in the Burgers picture) asymptotics forms the basis for the following analysis of the various phases.

We first discuss the strong-interference regime, $V(x) = 0$ and sufficiently strong $\theta(x)$, in section III. This is the regime most directly related to the NSS model and the Chalker-Coddington model described above. Naively, one may think in analogy to the case of classical disordered systems where $\theta(x) = 0$, that points of stationary phase take on the role of the local minima of the energy landscape, and dominate the partition sum. We will show that this is incorrect. Instead, fluctuations of $Z(w)$ along the entire system are important. In our analytical treatment using the replica formalism, this manifests itself as a pairing of replicas. We will see that there is a finite density of zeroes of $Z(w)$ (as already observed in [23]) which manifests itself in a logarithmic singularity of the effective disorder correlator $\Delta(w - w')$ for w close to w'.

In section IV, we consider the influence of random phases in the frozen regime (large $\beta V(x)$), where only a few local minima of the random potential contribute to $Z(w)$. In the $\beta \to \infty$ limit one finds sharp jumps between these minima as w is varied. In the Burgers velocity profile, these manifest themselves as shocks, and their statistics are known to be encoded in a linear cusp of the effective disorder correlator [15, 16]. We then discuss how the form of these shocks is modified by the introduction of random phases. It turns out that the linear cusp of the effective disorder correlator again acquires a logarithmic singularity. This time, however, it is related to shocks between two minima where the phase angle difference is π, i.e. $Z(w)$ passes through 0. This phenomenon is dependent on the spatial structure and on the possibility to vary w, and hence was not observed in [23].

In section V, for completeness we briefly discuss the high-temperature phase. Here, fluctuations of Z are small compared to its expectation value, and Z never becomes zero. As a consequence, the effective disorder correlators are regular everywhere, indicating that no shocks or poles occur in the Burgers velocity field.

At any finite system size $L \sim \frac{1}{m}$, there are blurred cross-overs between these phases as shown in figure 1. They become sharp transitions in the thermodynamic limit if the variance of θ and V is rescaled with the system size L as $\overline{V^2} \sim \overline{\theta^2} \sim \ln L$ [23]. Since we are interested in the behaviour of the disorder correlators deep inside each individual phase, we do not follow this path but instead choose the simpler scaling ~ 1 or $\sim L$. By doing this for V and θ individually, we can shrink all phases but one in the phase diagram to points respectively lines, and discuss each phase individually.

In conclusion, one significant physical result of our work is that the introduction of random phases has quite different effects depending on the real potential $V(x)$. If $V(x)$ is sufficiently strong so that the system is in the frozen phase, even weak random-phase disorder imme-

diately introduces zeroes of $Z(w)$ or turns the shocks of the real Burgers velocity profile into poles of the complex Burgers velocity profile. In the high-temperature phase, where $V(x)$ is weak, this does not happen for weak random phase disorder, and the effective disorder correlators remain analytic.

II. PRELIMINARIES

A. Definition of the model

To completely define the model (3), one needs to specify the joint distribution of the random potential $V(x)$ and the random phases $\theta(x)$. For the purpose of this paper, we assume that V and θ are independent, and that the distribution of θ is symmetric around 0. This is mostly for technical reasons (since this choice makes many observables real) and is certainly true e.g. for centered Gaussian distributions.

Typically, one chooses $V(x)$ to be Gaussian with mean zero, $\overline{V(x)} = 0$, and variance depending on the type of correlations. Here $\overline{\cdots}$ denotes averages over realizations of the disorder. In the absence of imaginary disorder, a short-range correlated $V(x)$, i.e. $\overline{V(x)V(x')} = 0$ unless $x = x'$, gives the so-called Kida model [17, 26, 27]. If one chooses $V(x)$ to be long-range correlated as a random walk, $\overline{[V(x) - V(x')]^2} \sim |x - x'|$, one obtains the Sinai model [28]. For $\theta(x)$ we also assume translationally invariant correlations.

For some computations, it is easier to regularise by a finite system size L,

$$Z_L := \frac{1}{L} \int_0^L e^{-\beta V(x) - i\theta(x)} \, \mathrm{d}x \; . \tag{4}$$

The system size L can be related to the mass of the harmonic well through $L \sim \frac{1}{m}$. In the case of pure random-phase disorder, i.e. $V(x) = 0$, (4) can be seen as a partition sum of a particle in the real random potential $\theta(x)$ at imaginary inverse temperature $i\beta$.

B. Proposed measurement of Z in cold atoms

A direct measurement of the partition sum as given in (3) for the strong-interference phase, i.e. with random phases $\theta(x)$ but without a random potential $V(x)$, is at least in principle possible in a cold-atom experiment: Prepare the system in the ground state of a weak harmonic well (with frequency ω), so that at $t = 0$ the wavefunction is

$$\psi_0(x) := \psi(x, t = 0) = \left(\frac{M\omega}{\pi\hbar}\right)^{\frac{1}{4}} e^{-\frac{M\omega x^2}{2\hbar}} \; . \tag{5}$$

Then, switch off the harmonic well, and instead switch on a random potential $\theta(x)$. In situations where the kinetic term in the Hamiltonian is negligible, such as $\omega t \ll 1$, or a large mass M, the time evolution is approximately given by $e^{-\frac{i}{\hbar}\theta(x)t}$, i.e.

$$\psi(x, t) = \left(\frac{M\omega}{\pi\hbar}\right)^{\frac{1}{4}} e^{-\frac{M\omega x^2}{2\hbar} - \frac{i}{\hbar}\theta(x)t} \; . \tag{6}$$

Switching the potential back to the harmonic well and measuring the overlap with the ground state gives

$$\langle\psi_0|\psi(t)\rangle = \left(\frac{M\omega}{\pi\hbar}\right)^{\frac{1}{2}} \int_{-\infty}^{\infty} \mathrm{d}x \, e^{-\frac{M\omega x^2}{\hbar} - \frac{i}{\hbar}\theta(x)t} \; . \tag{7}$$

This is exactly of the form of $Z(w)$ in (3) if one identifies $\frac{\beta m^2}{2} = \frac{M\omega}{\hbar}$. Although the overlap $\langle\psi_0|\psi(t)\rangle$ cannot be measured directly, the occupation probability of the ground state, given by $|\langle\psi_0|\psi(t)\rangle|^2$, could in principle be measured, providing a direct measurement of $|Z(0)|^2$ in the strong-interference regime. An example of a related experiment is given in [29].

C. Complex Burgers equation

Another application of the toy model (3) is to the complex Burgers equation. With the mapping $t := m^{-2}$, one obtains from (3) the "equation of motion" or "renormalisation group equation" (m^2 being interpreted as the infrared cutoff) for Z,

$$\partial_t Z(w, t) = \frac{T}{2}\partial_w^2 Z(w, t) \; . \tag{8}$$

We have added the argument t for clarity. The initial condition at $t = 0$ equivalent to $m^2 = \infty$ is

$$Z(w, 0) = e^{-\beta V(w) - i\theta(w)} \; . \tag{9}$$

Using the Cole-Hopf transformation $h(w, t) := -T \ln Z(w, t)$, we obtain the KPZ-equation

$$\partial_t h(w, t) = \frac{T}{2}\partial_w^2 h(w, t) - \frac{1}{2}\left[\partial_w h(w, t)\right]^2 \; . \tag{10}$$

Taking one spatial derivative one arrives at the Burgers equation for the velocity $u(w, t) := \partial_w h(w, t)$:

$$\partial_t u(w, t) = \frac{T}{2}\partial_w^2 u(w, t) - u\partial_w u(w, t) \; . \tag{11}$$

Without random phases ($\theta(x) = 0$), $u(w, t)$ is real and (11) is the well-studied *real* Burgers equation. It has been used, among others, to describe the formation of large-scale structures in cosmology (the so-called *adhesion model*) and in compressible fluid dynamics (for a review see [30]). When random phases are included, u becomes complex. The resulting complex Burgers equation has been used to obtain further information on the real Burgers equation through analytic continuation to

the complex plane and the so-called *pole expansion* [31–34].

However, it also has very surprising new applications e.g. to lozenge tilings of polygons [25]. For such tilings, the space and time directions of (11) become two coordinate axes in the plane. The random initial condition (9) at $t = 0$ (or $m = \infty$) in our model corresponds to fixing the height function of the tiling along a one-dimensional infinite boundary.

In the following, we study the small-m properties of (3), or equivalently the large-t properties of the complex Burgers equation (11). In the context of lozenge tilings, this corresponds to the limit of large distances from the boundary along which the height function is fixed by the random initial condition. We shall see that even in this limit, the roughness of the random initial condition (measured e.g. by the range of its correlations) influences the structure of the Burgers velocity field (see also the discussion in section VI).

D. Effective disorder correlators

The main observables on which we base our analysis are the so-called *effective disorder correlators*, which we define now. For each realization of the random potential $V(x)$ and the random phases $\theta(x)$, we first define the "free energy" or the "effective potential" by

$$\beta \hat{V}(w) + i\hat{\theta}(w) := \beta h(w) \equiv -\ln Z(w) . \qquad (12)$$

Note that $\hat{V}(w)$ is always unique, but $\hat{\theta}(w)$ is only defined modulo 2π. We will thus focus on $\hat{\theta}'(w)$ which is unambiguous. This is also the reason why it is preferable to consider the Burgers equation (11) instead of the equation (10) for the potential.

The effective disorder correlators for the potential and the phase are then defined by

$$\Delta_V(w_1 - w_2) := \overline{\hat{V}'(w_1)\hat{V}'(w_2)}$$
$$\Delta_\theta(w_1 - w_2) := \overline{\hat{\theta}'(w_1)\hat{\theta}'(w_2)} . \qquad (13)$$

The cross-correlator $\overline{\hat{V}'(w_1)\hat{\theta}'(w_2)}$ vanishes since $V(x)$ and $\theta(x)$ are independent and due to the symmetry $\theta \to -\theta$. In more general situations, this may not hold.

The correlators defined above have a nice representation as correlation functions. Define the normalized expectation value of an observable $\mathcal{O}$ for a given w as

$$\langle \mathcal{O}(x) \rangle_w := \frac{1}{Z(w)} \sqrt{\frac{\beta m^2}{2\pi}} \qquad (14)$$
$$\times \int_{-\infty}^{\infty} \mathrm{d}x \, e^{-\beta \left[V(x) + \frac{m^2}{2}(x-w)^2 \right] - i\theta(x)} \mathcal{O}(x) .$$

By definition $\langle 1 \rangle_w = 1$. Taking a derivative of (12) yields

$$-\frac{Z'(w)}{Z(w)} = \beta \hat{V}'(w) + i\hat{\theta}'(w) = \beta m^2 \langle w - x \rangle_w \qquad (15)$$

This gives two simple relations for Δ_V and Δ_θ:

$$\Delta_{ZZ}(w_1 - w_2) := m^4 \overline{\langle x - w_1 \rangle_{w_1} \langle x - w_2 \rangle_{w_2}} \qquad (16)$$
$$= \Delta_V(w_1 - w_2) - \beta^{-2} \Delta_\theta(w_1 - w_2)$$
$$\Delta_{ZZ^*}(w_1 - w_2) := m^4 \overline{\langle x - w_1 \rangle_{w_1} \langle x - w_2 \rangle_{w_2}^*} \qquad (17)$$
$$= \Delta_V(w_1 - w_2) + \beta^{-2} \Delta_\theta(w_1 - w_2)$$

In terms of the complex Burgers equation (11), the effective disorder correlators have the intuitive interpretation of equal-time velocity correlation functions:

$$\Delta_{ZZ}(w_1 - w_2) = \overline{u(w_1, t)u(w_2, t)}$$
$$\Delta_{ZZ^*}(w_1 - w_2) = \overline{u(w_1, t)u^*(w_2, t)}$$

The effective disorder correlator (17) has an interesting interpretation in the cold-atoms experiment proposed in section II B. Taking the overlap with the first excited state

$$\psi_1(x) = \frac{\sqrt{2}}{\pi^{\frac{1}{4}}} \left(\frac{M\omega}{\hbar} \right)^{\frac{3}{4}} x \, e^{-\frac{M\omega x^2}{2\hbar}} \qquad (18)$$

of the harmonic oscillator, instead of the ground state as in (7), we obtain

$$\langle \psi_1 | \psi(t) \rangle = \sqrt{\frac{M\omega}{\pi\hbar}} \sqrt{\frac{2M\omega}{\hbar}} \int_{-\infty}^{\infty} \mathrm{d}x \, x \, e^{-\frac{M\omega x^2}{\hbar} - \frac{i}{\hbar}\theta(x)t} . \qquad (19)$$

Thus, with the identification $\frac{\beta m^2}{2} = \frac{M\omega}{\hbar}$,

$$\langle \psi_0 | \psi(t) \rangle = Z(0)$$
$$\langle \psi_1 | \psi(t) \rangle = \frac{1}{\sqrt{\beta m^2}} Z'(0) .$$

Inserting this into (17) and using (15) gives

$$\Delta_{ZZ^*}(0) = \frac{1}{\beta^2} \overline{\frac{Z'(0)}{Z(0)} \frac{Z'(0)^*}{Z(0)^*}} = \frac{m^2}{\beta} \overline{\frac{|\langle \psi_1 | \psi(t) \rangle|^2}{|\langle \psi_0 | \psi(t) \rangle|^2}} . \qquad (20)$$

Thus, $\Delta_{ZZ^*}(0)$ is the average of the probability of a transition to the first excited state of the harmonic oscillator, divided by the probability of remaining in the ground state. In the following, we shall abbreviate this ratio as the *relative transition probability* to the first excited state. The average is a disorder average, but can likewise be implemented as an average over a large number of spatially well-separated harmonic traps.

We will now proceed with computing Δ_{ZZ} and Δ_{ZZ^*} explicitly in each of the three phases.

III. THE STRONG-INTERFERENCE PHASE (PHASE III)

The strong-interference phase has first been discussed in the context of directed paths with random complex weights in [19, 21, 35] and later for the random-energy

model at complex temperature [23]. In this phase, the average of Z is essentially zero (or at least subdominant) due to strong interference, and Z is dominated by fluctuations. The whole system contributes to the partition sum, in contrast to the case of a real random potential, where it is dominated by a few points with exceptionally large moduli.

In a replica formalism, this is reflected by a pairing of the replicas, as already observed for the NSS model in [35]. For the two-dimensional model discussed there, an entropic attraction between replica pairs arises at crossings of four or more replicas due to the spatial structure. In our one-dimensional model, the resulting replica pairs will turn out to be essentially non-interacting and spread out over the whole system.

We will analyze this phase by setting $V(x) = 0$ in (3) and consider the small-m limit. We shall show that: (i) this phase is characterized by $Z(w)$ being a Gaussian stochastic process in the complex plane with w as the time variable; (ii) its two-time correlation function is universal and given by

$$\overline{Z(w)Z(w')} \sim e^{-\frac{\beta m^2}{4}(w-w')^2} . \qquad (21)$$

From this, the effective disorder correlators defined above can be computed. We shall see that Δ_V and Δ_θ exhibit a logarithmic singularity around zero, describing the statistics of zeroes of Z. In contrast, $\Delta_{ZZ} = \Delta_V - \beta^{-2}\Delta_\theta$ remains regular around zero.

We then consider two explicit examples where the random phase disorder is sufficiently strong to observe this phase. Example 1 will be a model with Brownian imaginary disorder, i.e. long-range correlated phases $\overline{[\theta(x) - \theta(x')]^2} \sim |x - x'|$. Example 2 will be a model with short-range correlated phases uniformly distributed on $[-\pi, \pi[$.

A. Characterization of phase III and probability distribution of Z

We set $V(x) = 0$ in (3) and consider imaginary disorder. There is a large class of processes $\theta(x)$ such that in the limit $m \to 0$ the distribution of $Z(w)$ tends to a complex Gaussian variable due to a central limit theorem (CLT). To understand qualitatively why, let us think of $Z(w)$ as a discrete sum $Z(w) \approx \frac{1}{L}\sum_{j=1}^{L} z_j$ where each $z_j = e^{i\theta_j}$ is a random variable inside the unit disk and $L \sim 1/m$. The usual statement of the CLT shows that uncorrelated variables z_j belong to this class, (this is applied e.g. in example 2, section III E). In the more general case of correlated z_j a CLT also holds under the assumption that the correlations of the z_j decay fast enough. A precise mathematical statement of the necessary and sufficient conditions is possible using a so-called *strong mixing condition* (see [36–38]).

More qualitatively, we require the conditions that

$$q_\pm = \int_{-\infty}^{\infty} dx\, \overline{e^{i\theta(0)\pm i\theta(x)}} \qquad (22)$$

are finite and that a similar condition for the integral of the fourth cumulant holds. Since we assumed that $\theta(x)$ is symmetrically distributed around 0, the $q_\pm$ are real. Note that the fact that $Z(w)$ is bounded for any realization of $\theta(x)$ and any w by $|Z(w)| \le 1$ distinguishes this problem from the real potential case, where the CLT does not hold in general.

Thus, from now on we consider the case where the CLT holds and in the limit $m \to 0$ the distribution of $Z(w)$ tends to a complex Gaussian variable. This happens in what we call phases I and III. In these phases, the distribution of $Z(w)$ is thus determined by its mean $\overline{Z(w)}$ and its covariance matrix, consisting of 3 entries $\overline{Z(w)Z(w)}$, $\overline{Z(w)Z^*(w)}$, and $\overline{Z^*(w)Z^*(w)}$. A similar reasoning applies to the joint distribution of $Z(w)$ and $Z(w')$.

The key difference between the strong-interference phase III and the high-temperature phase I is the scaling of these moments: If the mean of Z as a function of m decreases faster than the fluctuations, $\overline{Z(w)}^2 \ll \overline{(Z(w) - \overline{Z(w)})^2} \sim m$ as $m \to 0$, we obtain the strong-interference, fluctuation-dominated phase III. If, on the other hand, the mean decreases slower than the fluctuations, $\overline{Z(w)}^2 \gg m$ as $m \to 0$, we obtain the high-temperature phase I.

In the example in section III D, we will take θ to be long-range correlated, $\overline{[\theta(x) - \theta(y)]^2} \sim |x - y|$, whence we will see that $\overline{Z(w)}^2 \sim e^{-\alpha/m} \ll m$. On the other hand, in section III E, we will consider an example where rotational symmetry enforces $\overline{Z(w)} = 0$. In both cases, we verify the general results and assumptions presented here.

B. The second moments

The second moments of the complex process $Z(w)$ take a general form which we derive now. The "renormalization-group" equation (8) describes how $Z(w)$ evolves under changes of $t = m^{-2}$. This implies a similar equation for the 2-point function $\tilde{f}(w - w') := \overline{Z(w)Z^*(w')}$,

$$\partial_t \tilde{f}_t(w) = T \partial_w^2 \tilde{f}_t(w) \qquad (23)$$

Here, we added the index t to make the dependence of $Z(w)$ on the parameter m and hence the dependence of $\tilde{f}(w)$ on the parameter t explicit. The general solution of (23) in terms of the initial condition $\tilde{f}_0(w) = \overline{e^{i(\theta(0) - \theta(w))}}$ is

$$\tilde{f}_t(w) = \sqrt{\frac{1}{4\pi T t}} \int_{-\infty}^{\infty} e^{-\frac{(w-w_0)^2}{4Tt}} \tilde{f}_0(w_0)\, dw_0 . \qquad (24)$$

Since we assumed q_- to be finite, see Eq. (22), the solution (24) tends to a Gaussian scaling form as $t \to \infty$

$$\tilde{f}_t(w) \to q_- \sqrt{\frac{1}{4\pi T t}} e^{-\frac{w^2}{4T t}} . \tag{25}$$

Note that this assumption is violated in phase I, where the mean $\overline{Z(w)}$ contributes a constant to $f_t(w)$ even for large t. It is also violated in phase II, where $\int_{-\infty}^{\infty} \tilde{f}_0(w_0) dw_0$ diverges.

Going back to the original variables m and β, the asymptotic form of (24) in phase III is

$$\tilde{f}_m(w - w') \xrightarrow{m \to 0} q_- \sqrt{\frac{\beta}{2\pi}} m f(\hat{w} = m\sqrt{\beta}(w - w')) \tag{26}$$

$$f(\hat{w}) = e^{-\frac{1}{4}\hat{w}^2} . \tag{27}$$

The scaling in (26) reflects the fluctuation-driven character of phase III: If the mean $\overline{Z(w)}$ were not subdominant, for large system sizes $L \sim m^{-1}$, as compared to the fluctuations, $\tilde{f}$ in (26) would be $\mathcal{O}(L^0)$ instead of $\mathcal{O}(L^{-1})$, and not tend to zero for large argument.

To summarize, in the strong-interference phase III, as $m \to 0$, the partition function $Z(w)$ tends to a Gaussian process with mean 0 and correlation matrix:

$$\begin{pmatrix} \overline{Z(w)Z(w)} & \overline{Z(w)Z^*(w)} & \overline{Z(w)Z(w')} & \overline{Z(w)Z^*(w')} \\ \overline{Z^*(w)Z(w)} & \overline{Z^*(w)Z^*(w)} & \overline{Z(w)Z(w')} & \overline{Z(w)Z^*(w')} \\ \overline{Z(w')Z(w)} & \overline{Z(w')Z^*(w)} & \overline{Z(w')Z(w')} & \overline{Z(w')Z^*(w')} \\ \overline{Z^*(w')Z(w)} & \overline{Z^*(w')Z^*(w)} & \overline{Z^*(w')Z(w')} & \overline{Z^*(w')Z^*(w')} \end{pmatrix} = m\sqrt{\frac{\beta}{2\pi}} \begin{pmatrix} q_+ & q_- & q_+ f(\hat{w}) & q_- f(\hat{w}) \\ q_- & q_+ & q_- f(\hat{w}) & q_+ f(\hat{w}) \\ q_+ f(\hat{w}) & q_- f(\hat{w}) & q_+ & q_- \\ q_- f(\hat{w}) & q_+ f(\hat{w}) & q_- & q_+ \end{pmatrix} \tag{28}$$

With this, we have completely characterized the $m \to 0$ asymptotics of $Z(w)$ in the strong-interference phase III as a Gaussian stochastic process with the second moment given by (26). In sections III D and III E we shall explicitly check the asymptotic form in (27) and obtain the non-universal constant $q_\pm$ in (27).

C. The disorder correlators

Having discussed the probability distribution of $Z(w)$, we now turn to computing the effective disorder correlators. For simplicity, we restrict ourselves to the case when the limiting Gaussian distribution for $Z(w)$ is rotationally symmetric, i.e. only depends on the modulus $|Z(w)|$. In the covariance matrix (28), this means $q_+ = 0$. The joint probability distribution for two partition sums $Z(w_1) = a_1 + i b_1$, and $Z(w_2) = a_2 + i b_2$ is then given by

$$P(a_1, b_1, a_2, b_2) = \frac{1}{4\pi^2 \sqrt{\det B}} e^{-\frac{1}{2}\vec{x}B^{-1}\vec{x}} , \tag{29}$$

with $\vec{x} = (a_1 \ b_1 \ a_2 \ b_2)$,

$$B = \frac{c}{2} \begin{pmatrix} 1 & 0 & f(\hat{w}) & 0 \\ 0 & 1 & 0 & f(\hat{w}) \\ f(\hat{w}) & 0 & 1 & 0 \\ 0 & f(\hat{w}) & 0 & 1 \end{pmatrix} , \tag{30}$$

and $c = mq_- \sqrt{\frac{\beta}{2\pi}}$. We will see later that the disorder correlator does not depend on c.

To compute the effective disorder correlators, let us reconsider their definition (13). Since $\hat{\theta}$ is the angular variable of a two-dimensional Gaussian stochastic process, we can apply the results of [17]. There, the two-time correlation function for the angular "velocity" $\dot{\hat{\theta}}(w) := \partial_w \hat{\theta}(w)$ of planar Brownian motion is (cf. [39], formula 17):

$$\overline{\dot{\hat{\theta}}(w)\dot{\hat{\theta}}(w')} = -\frac{1}{2} [\partial_w \partial_{w'} \ln f(\hat{w})] \ln (1 - f(\hat{w})^2) . \tag{31}$$

The two-point correlator of the phase (instead of its velocity) can then be written as a double integral of (31), but no explicit expression is known.

The two-point correlator of $\ln |Z| = \beta \hat{V}$ is obtained from the explicit form (29) for the two-time probability distribution as

$$\beta^2 \overline{\hat{V}(w)\hat{V}(w')} = \overline{\ln |Z(w)| \ln |Z(w')|}$$
$$= \int_{-\infty}^{\infty} \frac{1}{4\pi^2 \sqrt{\det B}} e^{-\frac{1}{2}\vec{x}B^{-1}\vec{x}} \ln |a_1 + i b_1| \ln |a_2 + i b_2|$$

with B given by (30). This integral can be computed exactly (γ_E denotes Euler's constant):

$$\beta^2 \overline{\hat{V}(w)\hat{V}(w')} = \frac{1}{4} \left[(\gamma_E - \ln c)^2 + \text{Li}_2(f(\hat{w})^2) \right] \tag{32}$$

Plugging in the scaling form $f(\hat{w}) = e^{-\frac{1}{4}\hat{w}^2}$ into (31) and

(32), we obtain the disorder correlators

$$\Delta_V(w) = -\frac{m^2}{4\beta}\left[\frac{\hat{w}^2}{e^{\frac{1}{2}\hat{w}^2}-1} + \ln\left(1 - e^{-\frac{1}{2}\hat{w}^2}\right)\right]$$

$$\Delta_\theta(w) = -\beta\frac{m^2}{4}\ln\left(1 - e^{-\frac{1}{2}\hat{w}^2}\right). \qquad (33)$$

Equivalently,

$$\Delta_{ZZ}(w) = -\frac{m^2}{4\beta}\frac{\hat{w}^2}{e^{\frac{1}{2}\hat{w}^2}-1} \qquad (34)$$

$$\Delta_{ZZ^*}(w) = -\frac{m^2}{4\beta}\left[\frac{\hat{w}^2}{e^{\frac{1}{2}\hat{w}^2}-1} + 2\ln\left(1 - e^{-\frac{1}{2}\hat{w}^2}\right)\right]. \qquad (35)$$

Observe that Δ_{ZZ} is smooth around 0, whereas Δ_{ZZ^*} has a logarithmic singularity at $w = 0$. Note that all correlators are expressed in terms of the rescaled variable $\hat{w}$ defined in (26).

The above expressions for the correlators (which are also the two-point equal-time velocity correlators for the complex Burgers equation) are universal and generally valid in phase III, under the assumption of rotationally invariant disorder. The more general case can be handled by similar methods but is not studied here. These results were obtained using the CLT assumption.

We now study two specific models where we can compute the general moments (beyond the second one) using the replica method, and check that they are consistent with the above reasoning. As an additional check we also compute numerically the correlators.

D.   Example 1: Imaginary Brownian disorder

Consider pure random-phase disorder, $V(x) = 0$, and take $\theta(x)$ to be a continuous random walk, i.e. a Gaussian stochastic process satisfying

$$\overline{[\theta(x) - \theta(x')]^2} = 2\sigma|x - x'|. \qquad (36)$$

Thus in the finite length regularization, the partition sum (4) is the Sinai model at an imaginary temperature. We measure numerically the effective disorder correlators, using relations (16) and (17). The results are compared in figure 2 against the analytic computation in the previous section. We observe good agreement.

1.   Second moment

Here we show explicitly the validity of the scaling argument given in section III B for this model.

Using formula (3), the second moment is given by

$$\overline{Z(w)Z^*(w')} \qquad (37)$$

$$= \frac{\beta m^2}{2\pi}\int_{-\infty}^{\infty} \mathrm{d}x\,\mathrm{d}y\,e^{-\frac{1}{2}\sigma|x-y|-\beta\frac{m^2}{2}\left[(x-w)^2+(y-w')^2\right]}$$
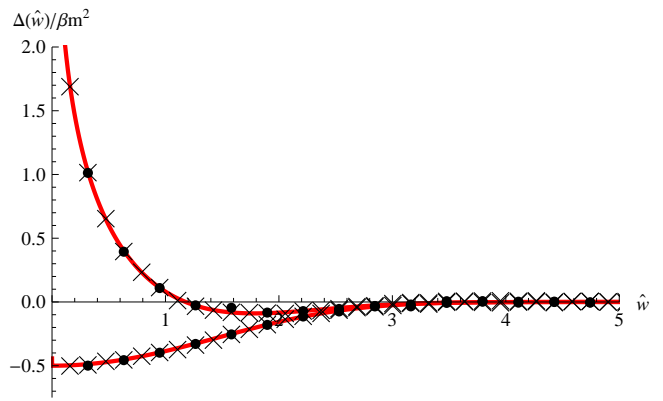

FIG. 2: Effective force-force correlators for the long-range model defined by (36). Lines (from top to bottom): Δ_{ZZ^*} from (35), Δ_{ZZ} from (34). Dots: corresponding correlators obtained numerically using (16) and (17) from $5\cdot10^5$ realizations of (3) with θ as in (36) for $\sigma = 1, \beta = 10$ and $m = 0.05$ (dots), $m = 0.1$ (crosses).

This integral (37) can be computed exactly by using the center-of-mass variable s and the "pair separation" variable t, defined as

$$s := \frac{x+y}{2}$$

$$t := x - y. \qquad (38)$$

In these variables, the s and t-integrals decouple,

$$\overline{Z(w)Z^*(w')} = \frac{\beta m^2}{2\pi}\left(\int_{-\infty}^{\infty}\mathrm{d}s\,e^{-\beta\frac{m^2}{2}\left[(s-w)^2+(s-w')^2\right]}\right)$$
$$\times\left(\int_{-\infty}^{\infty}\mathrm{d}t\,e^{-\frac{1}{2}\sigma|t|+\beta\frac{m^2}{2}(w-w')t-\beta\frac{m^2}{4}t^2}\right) \qquad (39)$$

Both integrals can be performed analytically. In terms of the rescaled variables

$$\hat{w} := m\sqrt{\beta}(w - w') \qquad (40)$$
$$\hat{\sigma} := \frac{\sigma}{m\sqrt{\beta}},$$

the second moment (39) is given by

$$\overline{Z(w)Z^*(w')} = \tfrac{1}{2}e^{-\frac{\hat{w}^2}{4}}\left[e^{\frac{(\hat{\sigma}-\hat{w})^2}{4}}\mathrm{Erfc}\left(\frac{\hat{\sigma}-\hat{w}}{2}\right)\right.$$
$$\left.+e^{\frac{(\hat{\sigma}+\hat{w})^2}{4}}\mathrm{Erfc}\left(\frac{\hat{\sigma}+\hat{w}}{2}\right)\right] \qquad (41)$$

Taking the $m \to 0$ limit at fixed β (i.e. the limit $\hat{\sigma} \to \infty$), the second moment (41) approaches the scaling form

$$\overline{Z(w)Z^*(w')} \sim \frac{2}{\sqrt{\pi}\hat{\sigma}}f(\hat{w})$$
$$f(\hat{w}) = e^{-\frac{1}{4}\hat{w}^2} \qquad (42)$$

This is exactly the scaling form obtained in (27), and gives a non-trivial check for the validity of that argument.

2. Higher moments

Let us now look at higher moments of Z and Z^*, given by:

$$\overline{Z(w_1)...Z(w_n)Z^*(w'_1)...Z^*(w'_n)}$$
$$= \int_{-\infty}^{\infty} \mathrm{d}x_1 \cdots \mathrm{d}x_n \int_{-\infty}^{\infty} \mathrm{d}y_1 \cdots \mathrm{d}y_n$$
$$\times e^{-\frac{\sigma}{4}\left[\sum_{i,j=1}^n |x_i-y_j|+|y_i-x_j|-|x_i-x_j|-|y_i-y_j|\right]}$$
$$\times e^{-\beta \frac{m^2}{2}\sum_{i=1}^n \left[(x_i-w_i)^2+(y_i-w'_i)^2\right]} \tag{43}$$

An exact calculation does not seem feasible, but the asymptotic behaviour is understood as follows: In the limit $\hat{\sigma} \to \infty$, the exponent in (43) will have a sharp maximum at configurations where the x_i and y_j are paired, i.e. close to each others. We now consider configurations which are close to such a pairing, where without loss of generality x_i is paired to $y_{\pi(i)}$ with some permutation π. Similar to (38) we introduce center-of-mass and separation coordinates s_i and t_i for each pair and rewrite the mass terms as in (39).

The t_i-integrals have complicated boundaries, which yield terms decaying as $e^{-\alpha\hat{\sigma}}$ with various functions $\alpha > 0$. Hence, these terms can be neglected in the limit $m \to 0$, and the s and t-integrals decouple again:

$$\overline{Z(w_1)...Z(w_n)Z^*(w'_1)...Z^*(w'_n)}$$
$$= \sum_\pi \prod_{i=1}^n \overline{Z(w_i)Z^*(w'_{\pi(i)})} + \text{ higher orders in } m \tag{44}$$

In particular, we get

$$\overline{[Z(w)Z^*(w')]^n} = n! \left[\overline{Z(w)Z^*(w')}\right]^n$$
$$+ \text{ higher orders in } m \tag{45}$$

A more rigorous justification that this is the leading term in an expansion in orders of m is given in appendix A by considering the moments of the partition sum in a finite system (4).

Correspondingly, the leading term for the moments $\overline{[Z(w)]^n [Z^*(w')]^m}$ for $m \neq n$ is zero in the strong-disorder limit, since then the replicas cannot be paired. Stated differently, the phase of Z is random, and hence only moments invariant under the rotation $Z \to e^{i\phi}Z$ are nonzero. Dropping the higher-order terms in (44), we obtain exactly the moments of a complex Gaussian variable. This supports the general claim made in section III A, and shows that this model is indeed in the strong-interference phase III.

The fact that configurations with unpaired replicas are subdominant shows that fluctuations of Z dominate over the average. Intuitively, this happens since for $\hat{\sigma} \gg 1$ the phase of the integrand in the expression (3) grows beyond 2π on a scale much smaller than the width $\frac{1}{m}$ of the parabolic well. Hence, (3) is essentially a sum of many random complex numbers with mean 0.
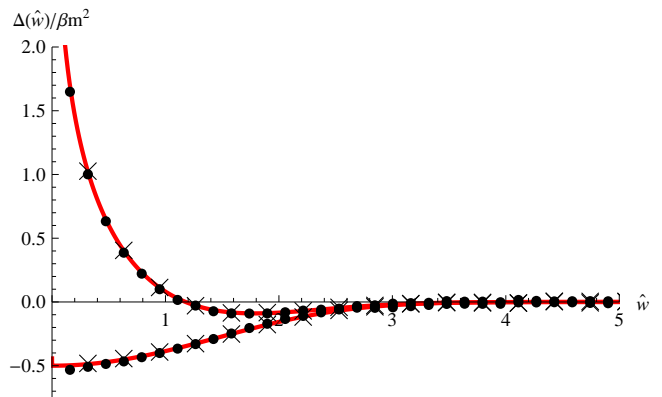

FIG. 3: Effective force-force correlators for the short-range model defined by (46). Lines (from top to bottom): Δ_{ZZ^*} from (35), Δ_{ZZ} from (34). Dots: corresponding correlators obtained numerically using (16) and (17) from $5 \cdot 10^5$ realizations of (3) with θ as in (46) for $\sigma = 1, \beta = 10$ and $m = 0.05$ (dots), $m = 0.1$ (crosses).

This is the same behaviour as in "phase III" discussed by Cook and Derrida [19] and by Derrida [23]. Since our potential is long-range correlated, $\overline{\theta(x)^2} \sim x$ instead of the short-range correlated potential $\overline{\theta(x)^2} \sim 1$ used in [19], the complex phase of the integrand in (3) grows much faster in our model. Hence, we do not observe "phase I" for high temperatures ($\beta < \beta_c$) as in [19, 23], but only the fluctuation-dominated "phase III".

In the following, we shall show that similar results hold in a model with uniformly distributed $\theta(x)$.

E. Example 2: A short-range correlated model with uniformly distributed angles

Our second example is a model, where the potential $\theta(x)$ in (4) is short-range correlated and uniformly distributed. To be more precise,

$$P\big(\theta(x)\big) = \frac{1}{2\pi} , \tag{46}$$

while $\theta(x)$ and $\theta(x')$ are uncorrelated for $x \neq x'$.

As can be seen on figure 3, a numerical simulation yields disorder correlators which compare well to the general results obtained above. As for the first example, we shall compute moments of Z to elucidate the physics.

Invariance of the distribution of $\theta(x)$ under a phase shift, $\theta(x) \to \theta(x) + \phi$, implies invariance of the distribution of Z under $Z \to Z\,e^{i\phi}$. Hence, the only nonzero moments are of the form $\overline{|Z(w)|^{2n}}$.

For $n = 1$, evaluating the second moment gives:

$$\overline{Z(w)Z^*(w')} =$$
$$= \frac{\beta m^2}{2\pi} \int_{-\infty}^{\infty} e^{-\beta \frac{m^2}{2}\left[(x-w)^2+(x-w')^2\right]} \overline{e^{-i[\theta(x)-\theta(x')]}}\, \mathrm{d}x\, \mathrm{d}x'$$
$$= \frac{\beta m^2}{2\pi} \int_{-\infty}^{\infty} e^{-\beta \frac{m^2}{2}\left[(x-w)^2+(x-w')^2\right]}\, \mathrm{d}x$$
$$= \sqrt{\frac{\beta m^2}{\pi}}\frac{1}{2} e^{-\beta \frac{m^2}{4}(w-w')^2} \tag{47}$$

Note that this is again in agreement with the general scaling argument given in section III B.

For the higher moments $\overline{[Z(w)Z^*(w')]^n}$, the only terms contributing are those where the $2n$ replica form n pairs. When at least two pairs are at the same position, it is not clear which replicas are pairs, leading to double-counting. However these contributions are subdominant and vanish with a relative factor of at least m^2. Thus, the dominant term for $m \to 0$ is

$$\overline{[Z(w)Z^*(w')]^n}$$
$$= n!\sqrt{\frac{\beta m^2}{2\pi}}^{2n} \left[\int_{-\infty}^{\infty} e^{-\beta \frac{m^2}{2}\left[(x-w)^2+(x-w')^2\right]}\mathrm{d}x\right]^n$$
$$= n!\left[\overline{Z(w)Z^*(w')}\right]^n + \text{higher orders in } m$$

Analogously to the derivation of (45) this formulas can be generalized to moments of Z with different positions.

Again, we observe the same behaviour of the moments as for a complex Gaussian. In total, in the limit of large m, we recover the same phase III results as in the long-range correlated model in section III D, and confirm the validity of the general arguments in the beginning of this section once more.

IV. THE FROZEN PHASE (PHASE II)

For large β and sufficiently strong potential $V(x)$, the modulus of the integrand in (3) has a very broad distribution. It is well-known that the partition sum (in the absence of the harmonic well) is then dominated by a few points, the minima of $V(x)$. This so-called *frozen* phase has been extensively studied in the absence of random phases by a variety of methods (replica symmetry breaking [27], functional renormalization group [17] and rigorous mathematical analysis [40])

Distributions of V where a frozen phase occurs in the model (3) in absence of complex phases include:

- Long-range correlated random potentials $V(x)$, i.e. $\overline{V(x)V(x')} = \sigma|x - x'|$. This is known as the *Sinai model*, which describes the diffusion of a random walker in a 1D random static force field [28, 41].

- Short-range correlated random potentials $V(x)$, i.e. $\overline{V(x)V(x')} = \sigma\delta(x - x')$, where the amplitude is

rescaled logarithmically with the system size, or m: $\sigma \sim -\ln m$. Freezing occurs below some critical temperature, $\beta > \beta_c$, analogously to the random energy model [40].

Among the most interesting features of the frozen phase is the appearance of jumps between distant minima of $V(x)$ as the position w of the harmonic well in (3) is varied [16, 42–44]. These correspond to shocks [30] under the mapping to the Burgers equation discussed in section II C. In the following, we will discuss how their structure is changed upon introduction of random complex phases $\theta(x)$, following the standard treatment [17, 45] for the case without random phases.

A. Complex shocks

Let us first consider a fixed realization of the random potential $V(x)$ and the random phases $\theta(x)$. For almost all w, the real part of the exponent, $V(x) + \frac{m^2}{2}(x - w)^2$ has, as a function of x, a single minimum at some value $x = x_m(w)$. Then, in the low-temperature limit (i.e. $\beta \to \infty$)

$$Z(w) = e^{-\beta V(x_m)-i\theta(x_m)-\beta \frac{m^2}{2}(x_m-w)^2} \tag{48}$$

and hence

$$\hat{V}(w) = V(x_m) + \frac{m^2}{2}(x_m - w)^2 \tag{49}$$
$$\hat{\theta}(w) = \theta(x_m) \tag{50}$$

The function $x_m(w)$ is constant over some range of w, but then jumps to a different value at $w = w^*$. Denoting the two solutions at w^* by x_1 and x_2, the necessary condition for a jump is

$$V(x_1) + \frac{m^2}{2}(x_1 - w^*)^2 = V(x_2) + \frac{m^2}{2}(x_2 - w^*)^2 \tag{51}$$

In terms of the effective potential $\hat{V}$, two parabolic sections given by (49) (with $w = w_1$ and w_2, respectively) meet at w^* with a linear cusp. The first derivative, $\hat{V}'(w)$, has a discontinuity at w^*.

So far, this is the same picture as has been established for purely real disorder long ago in the context of the Burgers equation [15, 30, 46]. There, the appearance of the shocks is succintly encoded [16, 17] in the effective force-force correlator $\Delta(w)$, which extends to the broader context of interfaces in random media. It has been computed and tested both numerically [47, 48] and experimentally [49]. It encodes the statistics of the shocks through a linear cusp at $w = 0$. At finite temperature β, the shock is smoothened in the so-called thermal boundary layer which extends on a scale $w \sim T = \beta^{-1}$ [50, 51].

The additional random phase $\theta(x)$ will in general be different at x_1 and x_2. We now show that this is reflected in the profile of $\hat{V}(w)$ and $\hat{\theta}(w)$ for w close to a shock.

This modifies the form of the disorder correlator $\Delta(w)$ near $w = 0$, more specifically in the thermal boundary layer region $w \sim T$ where we will obtain its precise form. We find that it adds a logarithmic singularity which depends on the statistics of the phase jumps.

1. The shock profile – general case

Let us assume a two-well picture, i.e. approximate $Z(w)$ by

$$Z(w) = e^{-\beta[V_1 + \frac{m^2}{2}(x_1 - w)^2] - i\theta_1} + e^{-\beta[V_2 + \frac{m^2}{2}(x_2 - w)^2] - i\theta_2} \tag{52}$$

The effective potential (12) can be written in terms of the jump size $s := \beta m^2 (x_2 - x_1)$, the phase difference, $\phi := \theta_2 - \theta_1$, and w^*, solution of (51):

$$\hat{\theta}'(w) = \frac{s}{2} \frac{\sin(\phi)}{\cos(\phi) + \cosh(s[w - w^*])} \tag{53}$$

$$-\hat{V}'(w) = \frac{s}{2\beta} \frac{\sinh(s[w - w^*])}{\cos(\phi) + \cosh(s[w - w^*])} \tag{54}$$
$$+ \frac{m^2}{2}(x_1 + x_2 - 2w)$$

Some examples of shock profiles for various values of the parameters are shown in figure 4. Note that as $\phi \to \pm\pi$, a pole appears in $\hat{V}'(w)$ at $w = w^*$ which is the real part of the Burgers velocity.

To obtain the disorder correlator Δ_θ, we need to average $\hat{\theta}'(w_1)\hat{\theta}'(w_2)$ over the disorder. Assume a small uniform density ρ_0 of shocks, and average over w^* with the measure $\rho_0 \int_{-\frac{1}{2\rho_0}}^{\frac{1}{2\rho_0}} \mathrm{d}w^*$. Since $\hat{\theta}'(w)$ decays rapidly as w^* is increased, we can safely extend the integration limits to $\pm\infty$, allowing to compute the integral over the shock position w^* analytically:

$$\Delta_\theta(w) = \rho_0 \int_{-\pi}^{\pi} \mathrm{d}\phi \int_0^\infty \mathrm{d}s\, P(\phi, s) f(\phi, s) \tag{55}$$

$$f(\phi, s) = s \sin^2(\phi) \frac{\phi \cot \phi - \frac{sw}{2} \coth \frac{sw}{2}}{\cos 2\phi - \cosh sw} \tag{56}$$

where $w = w_1 - w_2$. We denote by $P(\phi, s)$ the joint distribution of the jump sizes s and the phase jumps ϕ. Remarkably, $\Delta_V(w)$ can also be calculated, by considering the difference $\Delta_V(w) - \Delta_{V,\phi=0}(w)$, where $\Delta_{V,\phi=0}(w)$ is the correlator of the problem without the imaginary disorder, $\theta(x) = 0$:

$$\Delta_V(w) = \Delta_{V,\phi=0}(w) + \beta^{-2} \Delta_\theta(w) . \tag{57}$$

Thus the correlator $\Delta_{ZZ} = \Delta_V - \beta^{-2}\Delta_\theta$ is unchanged by the complex phases. Observe that the integrand in (55) becomes singular for $w = 0$ and $\phi = \pm\pi$. In the following examples (sections IV B and IV C) we shall see that this singularity yields a logarithmic singularity in $\Delta_{V,\theta}$ around zero. Its coefficient will be seen in section IV C to be proportional to $P(\phi = \pm\pi)$.
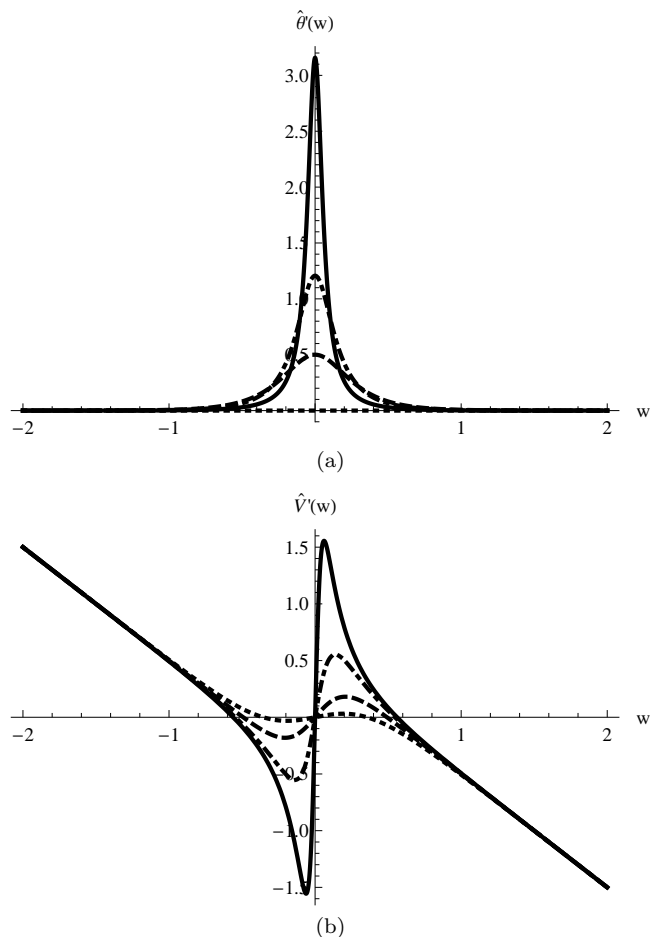

(a)

(b)

FIG. 4: Shock profiles from (54) for $\beta = 5$, $w^* = 0$, $x_1 + x_2 = 0$, $m = 1$ and $\phi = 0$ (dotted), $\phi = \frac{\pi}{2}$ (dashed), $\phi = \frac{3}{4}\pi$ (dot-dashed), $\phi = \frac{9}{10}\pi$ (solid).

We have now discussed the effective disorder correlators Δ_θ and Δ_V in a two-well approximation in a general situation. So far, we did not make specific assumptions on the distribution and the correlations of the disorder. These enter the final result (55) through the joint distribution of the jump sizes s and the phase jumps ϕ. Now, we will specialize to examples of particular interest.

B. Example 1: Uniformly distributed random phases in a short-range potential

Our first example is $\theta(x)$ uniformly distributed in $[-\pi, \pi]$ and uncorrelated from the spatial dependence x_i, i.e. $P(\phi, s) = \frac{1}{2\pi} P(s)$. This allows to perform the ϕ integral in (55) analytically:

$$\Delta_\theta(w) = \rho_0 \int_0^\infty \mathrm{d}s\, P(s) \frac{s}{2} \left[\frac{sw}{e^{sw} - 1} - \ln\left(1 - e^{-sw}\right) \right] \tag{58}$$

To take the limit $\beta \to \infty$, we write $s = \beta m^2(x_2 - x_1) = \beta m \mu \hat{s}$, where μ is the jump-size scale and the distribution
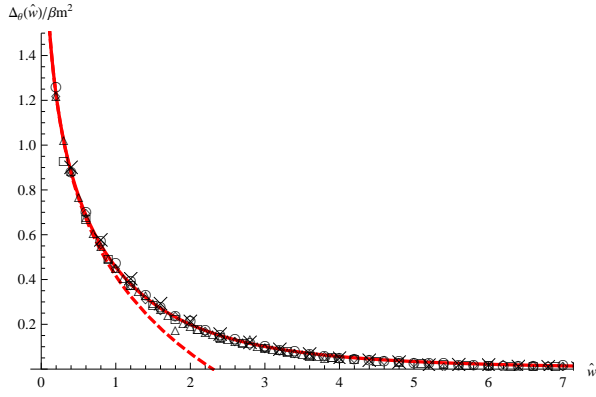
FIG. 5: (Color online) Correlator in phase II, with $\theta(x)$ uniform in $[-\pi, \pi]$. Dots: Numerical results using (16) and (17) from $1 \cdot 10^5$ realizations of (3) for $m = 0.01$, $\beta = 10$ (crosses), $m = 0.01$, $\beta = 20$ (circles), $m = 0.05$, $\beta = 20$ (triangles), $m = 0.05$, $\beta = 40$ (diamonds), $m = 0.05$, $\beta = 60$ (squares). Solid red (gray) line: (61), dashed red (gray) line: asymptotics (62). Rescaling was performed according to (61) with $\mu = 0.58$ (for all curves).

$P(\hat{s})$ is known as the Kida distribution [17, 26, 27],

$$P(\hat{s}) = \frac{1}{2} \hat{s} e^{-\frac{\hat{s}^2}{4}} \ . \tag{59}$$

The scale μ is related to the density of shocks ρ_0 through [17]

$$1 = \rho_0 \langle x_2 - x_1 \rangle = \rho_0 \frac{\mu}{m} \int_0^\infty \mathrm{d}\hat{s}\, P(\hat{s}) \hat{s} = \rho_0 \frac{\mu}{m} \sqrt{\pi} \ . \tag{60}$$

We thus obtain the scaling form

$$\Delta_\theta(w) = \beta m^2 \tilde{\Delta}_\theta \left(\hat{w} = \beta m \mu w \right) \tag{61}$$

$$\tilde{\Delta}_\theta(x) = \int_0^\infty \mathrm{d}\hat{s}\, \frac{\hat{s}^2}{4\sqrt{\pi}} e^{-\frac{\hat{s}^2}{4}} \left[\frac{\hat{s}x}{e^{\hat{s}x} - 1} - \ln \left(1 - e^{-\hat{s}x} \right) \right] \ .$$

Observe that the scaling is different compared to the correlator in the strong-interference phase III: The argument of the scaling function is now $\hat{w} = \beta m \mu w$ instead of $\hat{w} = \sqrt{\beta} m w$ in (33).

For small x, (61) has the asymptotic form

$$\tilde{\Delta}_\theta(x) = \frac{1}{4}(\gamma_{\mathrm{E}} - 2 \ln x) + \mathcal{O}(x) \tag{62}$$

This logarithmic singularity arises from the $\phi = \pm\pi$ limit of the integral (55), and is hence caused by shocks where $Z(w^*) = 0$.

The integral (61) can be computed numerically and compared to simulations. We obtain a very good agreement with our numerical results (see figure 5) for various values of m and β, providing a non-trivial check for the scaling in (61). The scale μ is fitted as $\mu = 0.58$, independent of m or β in the considered range [1].

---

[1] Actually, for the short-range random potential on a discrete lat-

C. Example 2: Wrapped gaussian distribution in a short-range potential

It is interesting to consider an example where the distribution for ϕ is non-uniform. We take again the phase angle $\theta(x)$ to be uncorrelated at different points. At each point, we assume the distribution of $\theta \in [-\pi; \pi]$ to be a wrapped gaussian distribution with variance σ^2:

$$\tilde{P}(\theta) = \sqrt{\frac{1}{2\pi\sigma^2}} \sum_{n=-\infty}^{\infty} e^{-\frac{1}{2\sigma^2}(\theta + 2\pi n)^2} \tag{63}$$

$$= \sqrt{\frac{1}{2\pi\sigma^2}} e^{-\frac{1}{2\sigma^2}\theta^2} \vartheta \left(\frac{\theta}{\sigma^2}i; \frac{2\pi i}{\sigma^2} \right)$$

ϑ denotes the Jacobi theta function. Note that $\tilde{P}(\theta)$ is periodic, $\tilde{P}(\theta + 2\pi) = \tilde{P}(\theta)$. From (63), the distribution of phase jumps $\phi = \theta_2 - \theta_1$ is

$$P(\phi) = \int_{-\pi}^{\pi} \tilde{P}(\theta) \tilde{P}(\theta + \phi) \,\mathrm{d}\theta \ . \tag{64}$$

For the random potential, we still assume a short-range random potential as in section IV B. The distribution of jump sizes $\hat{s}$ is thus still given by (59). This allows to obtain the full disorder correlator Δ_θ by computing the integral (55) numerically. The results in figure 6 compare well to numerical simulations.

One again observes a distinctive logarithmic singularity at $w = 0$. This arises from the $\phi = \pm\pi$ limit of the integral (55). More precisely,

$$\int_{-\pi}^{\pi} \mathrm{d}\phi\, P(\phi) \sin^2(\phi) \frac{\phi \cot \phi - \frac{sw}{2} \coth \frac{sw}{2}}{\cos 2\phi - \cosh sw}$$

$$= -\pi P(\phi = \pm\pi) \ln w + \mathcal{O}(w^0) \tag{65}$$

The integral over $\hat{s}$ is normalized since $\int_0^\infty \frac{\hat{s}^2}{2\sqrt{\pi}} e^{-\hat{s}^2/4} \,\mathrm{d}\hat{s} = 1$, and hence

$$\tilde{\Delta}_\theta(x) = -\pi P(\phi = \pm\pi) \ln x + \mathcal{O}(x^0) \ . \tag{66}$$

For a uniform distribution of θ, $P(\phi = \pm\pi) = \frac{1}{2\pi}$ and we recover the ln part of the result (62). The constant coefficient of order w^0 is harder to obtain.

In general, the coefficient of the logarithmic singularity at $w = 0$ is proportional to the probability of phase jumps by an angle of $\phi = \pm\pi$. Thus intuitively this singularity is caused by shocks between minima of $V(x)$, where $Z(w^* - 0^+)$ changes to $Z(w^* + 0^+) = -kZ(w^* - 0^+)$ where k is a positive number. Note that at any temperature $T > 0$, i.e. $\beta < \infty$ the function $Z(w)$ is smooth, thus passes through zero in our two-well approximation. This means

---

tice considered here, μ contains corrections, which are scaling logarithmically with m; see [17] for more details. If we were to perform the simulations with m varying over several decades, μ would have to be adjusted correspondingly.
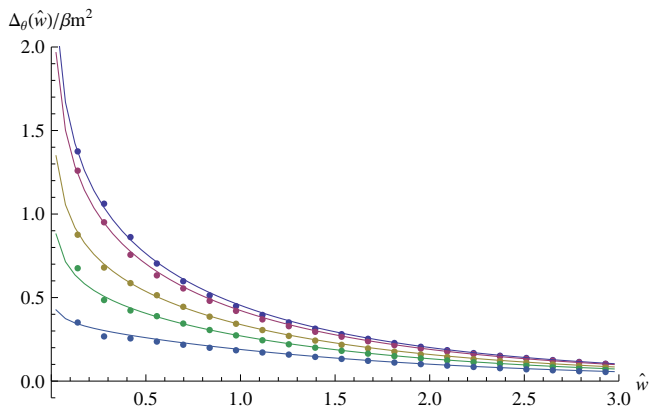
FIG. 6: Correlator in phase 2, with $\theta(x)$ wrapped gaussian as in (63). Dots: simulations (From top to bottom the variance decreases as: $\sigma = 2$, $\sigma = 1.6$, $\sigma = 1.2$, $\sigma = 1$, $\sigma = 0.8$, the mass is $m = 0.01$, and $\beta = 120$. Correspondingly, the probability of a jump through zero decreases as $P(\phi = \pm\pi) = 0.15, 0.13, 0.08, 0.05, 0.01$.), rescaled as in (61) with $\mu = 0.59$ (for all curves). Lines: numerical integration of (55).

that the Burgers velocity profile has a pole. Observe that according to (66), the logarithmic singularity is present as soon as there is a finite probability of jumps with an angle of $\phi = \pm\pi$, however small it may be. This shows that in our model, there is no "sign phase transition" in the frozen, or pinned phase. This is in agreement with a recent result for a higher-dimensional model [52] where only $\theta = 0$ and $\theta = \pi$, i.e. plus and minus signs were considered.

It is straightforward to repeat the analysis above with long-range correlated random potentials $V(x)$. For example, in the case of the Sinai model explicit expressions for the probability distribution (59) for the jump sizes s are known (see [17]) but lead to complicated integrals.

Note that the two-well model is only expected to be valid asymptotically for $\beta \to \infty$. At low but non-zero temperature, we expect subdominant contributions from higher-lying minima which may provide additional rounding of the singularities discussed above.

In the following, we shall see that the behaviour in the high-temperature phase is quite different.

V. THE HIGH-TEMPERATURE PHASE (PHASE I)

For completeness, we also discuss the disorder correlators in the high-temperature phase. In this phase Z is dominated by the average $\overline{Z}$, and fluctuations are subdominant. As a consequence, for example the quenched average of the free energy is equal to the annealed average of the free energy.

In our one-dimensional model, this phase occurs for sufficiently weak random potentials (for example, short-range correlated $V(x)$ below a critical value of β, which

increases with system size) and sufficiently weak random-phase disorder (for example, short-range correlated $\theta(x)$ with finite variance, e.g. a wrapped Gaussian distribution).

To compute the leading-order term for the correlators, let us take the example of short-range real and imaginary disorder, with

$$\overline{V(x)} = \overline{\theta(x)} = 0 \tag{67}$$

$$\overline{V(x)V(x')} = \sigma_V \delta(x - x') \tag{68}$$

$$\overline{\theta(x)\theta(x')} = \sigma_\theta \delta(x - x') \tag{69}$$

For small σ_V and σ_θ, we can expand the partition sum in powers of V and θ:

$$Z(w) \tag{70}$$

$$= \sqrt{\frac{\beta m^2}{2\pi}} \int_{-\infty}^{\infty} \mathrm{d}x \, [1 - \beta V(x) - i\theta(x) + ...] e^{-\beta \frac{m^2}{2}(x-w)^2}$$

The leading order for the effective potential thus becomes:

$$\hat{V}(w) = \sqrt{\frac{\beta m^2}{2\pi}} \int_{-\infty}^{\infty} V(x) e^{-\beta \frac{m^2}{2}(x-w)^2} \, \mathrm{d}x \tag{71}$$

$$\hat{\theta}(w) = \sqrt{\frac{\beta m^2}{2\pi}} \int_{-\infty}^{\infty} \theta(x) e^{-\beta \frac{m^2}{2}(x-w)^2} \, \mathrm{d}x \tag{72}$$

From this, we obtain the leading order for the disorder correlators in the high-temperature phase:

$$\Delta_V(w) = \sigma_V \frac{(\beta m^2)^{\frac{3}{2}}}{8\sqrt{\pi}} \left(2 - \hat{w}^2\right) e^{-\frac{\hat{w}^2}{4}} \tag{73}$$

$$\Delta_\theta(w) = \sigma_\theta \frac{(\beta m^2)^{\frac{3}{2}}}{8\sqrt{\pi}} \left(2 - \hat{w}^2\right) e^{-\frac{\hat{w}^2}{4}} \tag{74}$$

Here, $\hat{w} = m\sqrt{\beta}w$.

Another way to understand these correlators is through the so-called *exact renormalization group* equations following [17]. From (12) and (3), we obtain a flow equation of the form:

$$-m\partial_m \hat{V}(w) = \frac{1}{\beta m^2}\partial_w^2 \hat{V}(w) - \frac{1}{m^2}\left(\partial_w \hat{V}(w)\right)^2 \tag{75}$$

For the correlator $R(w - w') := \overline{\hat{V}(w)\hat{V}(w')}$, this gives:

$$-m\partial_m R(w) = \frac{2}{\beta m^2}\partial_w^2 R(w) + \frac{2}{m^2}S_{110}(0, 0, w) \tag{76}$$

Here, $S(w_1, w_2, w_3) := \overline{\hat{V}(w_1)\hat{V}(w_2)\hat{V}(w_3)}$ is the third cumulant and the subscript S_{110} indicates derivatives with respect to the first two arguments (notations as in [17]). Without the non-linear term, equation (76) is the same as (23), solved by (25) with initial conditions (68), i.e.

$$R(w) = \sigma_V \sqrt{\frac{\beta m^2}{4\pi}} e^{-\frac{\hat{w}^2}{4}} \tag{77}$$
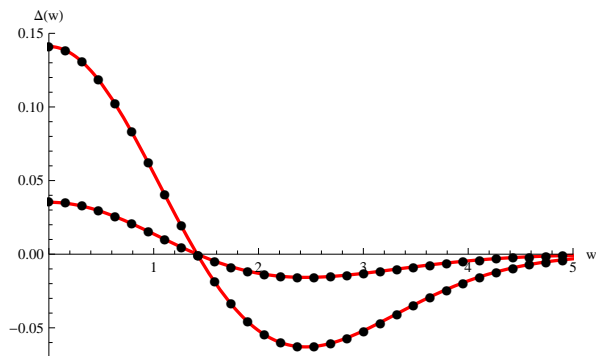
FIG. 7: (Color online) Renormalized disorder correlators in the high-temperature phase. Dots: Numerical results from $1 \cdot 10^5$ realizations of (3) for $\beta = 0.1, \sigma_V = 1, \sigma_\theta = 0.25, m = 0.5$. Solid red (gray) lines (from top to bottom): Δ_V, Δ_θ, as obtained from (73). No fit parameter.

The feeding term for S is of order $RR \sim \beta$, thus subdominant in β for high T, and (77) is the complete solution. Taking two derivatives one obtains $\Delta_V(w) = -\partial_w^2 R(w)$ in agreement with (73).

These results can be compared to simulations in the high-temperature region. As can be seen on figure 7, they show excellent agreement.

We thus observe that the behaviour of the model when random phases are added is very different in the high-temperature phase from what was observed in the frozen phase (section IV). For small random phase disorder, i.e. small σ_θ, the disorder correlators stay regular at zero and do not develop any cusp or logarithmic singularity. An intuitive, physical explanation for this can be given: In the high-temperature phase, the fluctuations of Z are subdominant compared to the average $\overline{Z}$ in the $m \to 0$ limit. Hence, even if there is a finite probability for fluctuations with opposite phases, a macroscopic number of them would need to occur simultenously in order to cancel the average $\overline{Z}$ and lead to a zero of $Z(w)$. This becomes infinitely improbable in the $m \to 0$ limit. On the other hand, in the frozen phase, Z can be approximated by a two-well picture, even in the $m \to 0$ limit. Then there is a finite probability for the two minima to have opposite phases, and thus a finite probability for a shock where Z passes through zero.

VI. SUMMARY AND CONCLUSION

In this paper, we have discussed interference effects in toy models of disordered systems. We considered one-dimensional models, where interference is included through a random complex phase on each lattice site.

We have obtained the scaling behaviour and asymptotic analytic expressions for the effective disorder correlators in the three phases of the model. For high temperatures small random phases do not change the physics, but strong random-phase disorder leads to a new strong-interference phase. This phase is characterized by a Gaussian distribution of Z centered around zero, and hence a finite density of zeroes of Z. For low temperatures, the system is frozen. Introducing random phases changes the structure of the shocks which are observed when a particle is "dragged" through the random potential. There, also, zeroes of Z or, equivalently, poles of the complex Burgers velocity field can occur. This physical characterization is seen in the effective disorder correlators as a logarithmic singularity around zero.

In the proposed realization of our model in a cold-atom experiment (section II B), the real part of the disorder is zero and hence only phases I and III can be observed. (20) allows us to interpret the results from sections V and III in this context: In phase I, where no shocks occur, $\Delta_{ZZ^*}(0)$ is finite (cf. (73)). Hence, the relative transition probability to the first excited state is finite. On the other hand, in phase III, $\Delta_{ZZ^*}(0)$ diverges logarithmically (cf. (35)), and so does the relative transition probability to the first excited state. This means that for sufficiently strong disorder (in the sense that it satisfies the criteria for phase III), in some realizations even after a short time the occupation probability of the ground state is zero while the occupation probability of the first excited state is finite. This consequence of our preceding analysis on phases I and III of the toy model may possibly even be verified experimentally.

In the applications to lozenge tilings discussed in section II C, shocks of the complex Burgers equation manifest themselves as boundaries between *frozen* regions of the tiling (where the orientation of the tiles is fixed uniquely, and the height function is flat) and *liquid* regions of the tiling (where the orientation of the tiles is not fixed uniquely, and the height function has a nontrivial, curved limiting shape) [25, 53]. Our results lead to the hypothesis that different roughness of the tiling boundary leads to different behaviour far away from it. One possibility is that frozen and liquid regions can both persist, implying the presence of shocks akin to phases II or III in our toy model. Intuitively, we expect this to happen for sufficiently rough boundaries. Another possibility is that no shocks occur for large distances from the tiling boundary, meaning that only a liquid region remains. We expect this to occur for weakly disordered boundaries, i.e. some version of the high-temperature phase I. Unfortunately, the results of our toy model do not directly allow a classification of this kind, since the distribution of $V(x)$ and $\theta(x)$ required to model a random tiling boundary is more complicated than the ones we restrict ourselves to in II and in the rest of the paper. However, elucidating the details of this connection and verifying this hypothesis would be an interesting field for further work.

A few other directions in which the present discussion could be continued come to mind. The most physically important aspect would be, certainly, to relate the phenomena observed here to higher-dimensional, more realistic models of interfering quantum systems. In principle,

one should be able to obtain the effective disorder correlators from field theory, in the frozen phase e.g. from functional renormalization group methods [5]. The main technical difficulty, as apparent from our toy model and a preliminary study [54] is the behaviour at zero: Instead of a rounding of the linear cusp at finite temperature, we may see a logarithmic singularity. This makes the derivation of a field theory for the frozen phase in the presence of random phases a challenging problem.

Another direction, which would be interesting to understand better, is the relationship of the present results on the abundance of poles of the Burgers velocity profile to the pole expansion method for the solution of the Burgers equation [31–34], and the pole condensation phenomena observed in [33].

Note added:

After completion of this paper we became aware of a very recent preprint [55] by Gredat, Dornier and Luck which also treats imaginary Brownian disorder motivated by a connection to reaction-diffusion processes. While the focus is different, i.e. they study the so-called Kesten variable which amounts to a linear potential regularization, while we study a quadratic well, there is agreement whenever the results can be compared.

Appendix A: Moments of the partition sum with finite system size L and long-range correlated disorder

Let us consider (4) with $V(x) = 0$ and $\theta(x)$ as defined in (36). In this appendix, we calculate explicitly moments of Z_L. We also discuss how they can be organized to extract the dominant contributions for large L.

First, we need to make some technical remarks. Consider the integral

$$I_n^L(\lambda_1, ..., \lambda_n) := \int_0^L dx_1 \ldots \int_0^{x_{n-1}} dx_n \, e^{\sum_{i=1}^n \lambda_i x_i} \quad \text{(A1)}$$

$$= \sum_{k=0}^n e^{\sum_{j=1}^k \lambda_j L} (-1)^{n-k} \prod_{l=1}^k \frac{1}{\sum_{j=l}^k \lambda_j} \prod_{l=k+1}^n \frac{1}{\sum_{j=k+1}^l \lambda_j}$$

By introducing the partial sums $\mu_k := \sum_{j=1}^k \lambda_j$, the for-

mula (A1) can be rewritten as

$$I_n^L(\lambda_j) = \sum_{k=0}^n e^{\mu_k L} \prod_{\substack{l=0 \\ l \neq k}}^n \frac{1}{\mu_k - \mu_l} \quad \text{(A2)}$$

Taking a Laplace transform with respect to L, this is further simplified to

$$\begin{aligned} \mathrm{LT}\{I_n(\lambda_j)\}(s) &= \int_{L=0}^\infty e^{-sL} I_n^L(\lambda_j) \, dL \\ &= I_{n+1}^\infty(-s, \lambda_1, \ldots, \lambda_n) \\ &= \prod_{l=0}^n \frac{1}{s - \mu_l} \end{aligned} \quad \text{(A3)}$$

Let us now return to the moments of ZZ^*. We would like to evaluate

$$\overline{(ZZ^*)^n} = \int_0^L dx_1 \cdots \int_0^L dx_n \int_0^L dy_1 \cdots \int_0^L dy_n$$
$$e^{-\frac{\sigma}{4}\left(\sum_{i,j=1}^n |x_i - y_j| + |y_i - x_j| - |x_i - x_j| - |y_i - y_j|\right)}$$

If we assume an ordering of the $2n$ variables x_j and y_j, the exponent is a linear combination of these variables. Hence, it is of the form of the integral (A1). Each ordering of the x's and y's can be mapped bijectively to a directed path from the lower left to the upper right corner in a $n \times n$ lattice: The choice of an x corresponds to going up, the choice of a y to going right[2].

Each ordering Σ can be defined by a vector Σ^x with $2n$ entries given by

$$\Sigma_j^x = \begin{cases} 1 & \text{if } j\text{th variable is } x \\ 0 & \text{if } j\text{th variable is } y \end{cases}, \quad \text{(A4)}$$

or equivalently by a vector Σ^y with $2n$ entries

$$\Sigma_j^y = \begin{cases} 1 & \text{if } j\text{th variable is } y \\ 0 & \text{if } j\text{th variable is } x \end{cases}. \quad \text{(A5)}$$

Then, the resulting values of the λ_j for the ordering Σ in the definition (A1) are

$$\frac{2}{\sigma} \lambda_j^\Sigma = (-1)^{\Sigma_j^x} \left[2 \left(\sum_{l=1}^j \Sigma_j^x - \sum_{l=1}^{j-1} \Sigma_j^y \right) - 1 \right] \quad \text{(A6)}$$

A few examples for $n = 2$ and $n = 3$ are given in table I. In order to apply (A2), we need the partial sums μ_k:

$$\begin{aligned} \frac{2}{\sigma} \mu_k^\Sigma &:= \frac{2}{\sigma} \sum_{j=1}^k \lambda_j = \sum_{j=1}^k (-1)^{\Sigma_j^x} \left[2 \left(\sum_{l=1}^j \Sigma_j^x - \sum_{l=1}^{j-1} \Sigma_j^y \right) - 1 \right] \\ &= - \left[\sum_{l=1}^k \left(\Sigma_j^x - \Sigma_j^y \right) \right]^2 \end{aligned} \quad \text{(A7)}$$

_____

[2] This generalizes straightforwardly to general moments like $Z^n (Z^*)^m$, which give directed paths on an $n \times m$ lattice.

Ordering	$\frac{2}{\sigma}\lambda_j$	$\frac{2}{\sigma}\mu_j$
xyxy	(-1,1,-1,1)	(0,-1,0,-1,0)
xyyx	(-1,1,-1,1)	(0,-1,0,-1,0)
xxyy	(-1,-3,3,1)	(0,-1,-4,-1,0)
xyxyxy	(-1,1,-1,1,-1,1)	(0,-1,0,-1,0,-1,0)
xyxxyy	(-1,1,-1,-3,3,1)	(0,-1,0,-1,-4,-1,0)
xxxyyy	(-1,-3,-5,5,3,1)	(0,-1,-4,-9,-4,-1,0)

TABLE I: The λ_j and μ_j for some orderings Σ.

Again, see table I for a few examples.

Using formula (A3), the the Laplace transform of the moments can be written as:

$$\overline{(ZZ^*)^n} = (n!)^2 \sum_\Sigma I_{2n}(\lambda_j^\Sigma) = (n!)^2 \sum_\Sigma \prod_{l=0}^{2n} \frac{1}{s - \mu_l^\Sigma} \tag{A8}$$

In the interpretation of Σ as a directed path $\Gamma = (w_0, \ldots, w_{2n})$, with w_j on the square $n \times n$ lattice and $w_0 = (0,0)$, $w_{2n} = (n,n)$, the formula (A7) obtains a direct interpretation: $\frac{2}{\sigma}\mu_k^\Sigma$ is $-d^2$, with d the distance to the diagonal. We thus obtain the interesting formula (setting $\sigma = 2$ for simplicity in the following):

$$\overline{(ZZ^*)^n} = (n!)^2 \sum_{\substack{\Gamma \\ \text{path } (0,0) \to (n,n)}} \prod_{w \in \Gamma} \frac{1}{s + d_w^2} \tag{A9}$$

with d_w the distance of w to the diagonal.

For the inverse Laplace transform, no closed formula is evident. However, from (A9) we can observe the following:

- The Laplace transform of $(ZZ^*)^n$ has poles at $s = 0$, $s = -1$, $s = -4$, $s = -9$, etc. Hence, $(ZZ^*)^n$ as a function of L can be written as a sum of terms of order 1, e^{-L}, e^{-4L}, e^{-9L}, etc.

- For large system sizes, the terms suppressed exponentially with L are irrelevant, and hence only the pole at $s = 0$ needs to be discussed.

- For each path, the pole at $s = 0$ has the form $\frac{1}{s^{z+1}}$ where z is the number of crossings of the diagonal. Its Laplace transform yields $\frac{L^z}{z!}$. Hence, the dominant term for large L is given by the paths with the maximum number of diagonal crossings.

- These are exactly the paths where the x_i and y_i are paired, i.e. xyxyxyxy... or xyyxxyxy... etc. There are 2^n such configurations.

The final result is

$$\overline{(ZZ^*)^n} = n!(2L)^n + \mathcal{O}(L^{n-1}) + \mathcal{O}(e^{-L})$$

This argument provides a somewhat more detailed explanation of why the only configurations contributing to moments of the form $(ZZ^*)^n$ are those where the replica are pairwise bound. When regularising the system by a harmonic well with mass m, we expect similar results, with – morally speaking – L replaced by $\frac{1}{m}$. However, we have not found a way to perform a more detailed computation using the regularization with a mass.

[1] K. Binder and A.P. Young, *Spin glasses: Experimental facts, theoretical concepts, and open questions*, Rev. Mod. Phys. **58** (1986) 801.

[2] A.P. Young, *Spin glasses and random fields*, World Scientific, Singapore, 1997.

[3] D. S. Fisher, *Interface fluctuations in disordered systems: 5-ϵ expansion and failure of dimensional reduction*, Phys. Rev. Lett. **56** (1986) 1964–1967.

[4] L. Balents and D. S. Fisher, *Large-n expansion of (4-ϵ)-dimensional oriented manifolds in random media*, Phys. Rev. B **48** (1993) 5949–5963.

[5] P. Le Doussal, K. J. Wiese and P. Chauve, *Functional renormalization group and the field theory of disordered elastic systems*, Phys. Rev. E **69** (2004) 26112.

[6] V. L. Nguyen, B. Z. Spivak and B. I. Shklovskii, *Tunnel hopping in disordered systems*, Sov. Phys. JETP **62** (1985) 1021–1029.

[7] E. Medina and M. Kardar, *Spin-orbit scattering and magnetoconductance of strongly localized electrons*, Phys. Rev. Lett. **66** (1991) 3187–3190.

[8] E. Medina and M. Kardar, *Quantum interference effects for strongly localized electrons*, Phys. Rev. B **46** (1992) 9984–10006.

[9] E. Medina, M. Kardar, Y. Shapir and X. R. Wang, *Magnetic-field effects on strongly localized electrons*, Phys. Rev. Lett. **64** (1990) 1816–1819.

[10] A. M. Somoza, M. Ortuño and J. Prior, *Universal distribution functions in two-dimensional localized systems*, Phys. Rev. Lett. **99** (2007) 1–4.

[11] J. Prior, A. M. Somoza and M. Ortuño, *Conductance distribution in two-dimensional localized systems with and without magnetic fields*, The European Physical Journal B **70** (2009) 513–521.

[12] J. T. Chalker and P. Coddington, *Percolation, quantum tunnelling and the integer hall effect*, Journal of Physics C: Solid State **2665** (1988).

[13] J. Cardy, *Quantum network models and classical localization problems*, International Journal of Modern Physics B **24** (2010) 1989.

[14] E. Beamond, J. Cardy and J. Chalker, *Quantum and classical localization, the spin quantum hall effect, and generalizations*, Phys. Rev. B **65** (2002) 214301.

[15] L. Balents, J.P. Bouchaud and M. Mézard, *The large scale energy landscape of randomly pinned objects*, J. Phys. I (France) **6** (1996) 1007–20.

[16] P. Le Doussal, *Finite-temperature functional RG, droplets and decaying Burgers turbulence*, Europhys. Lett. **76** (2006) 457.

[17] P. Le Doussal, *Exact results and open questions in first principle functional RG*, Ann. Phys. (2009) 1–98.

[18] P. P. Mitra and P. Le Doussal, *Long-time magnetization relaxation of spins diffusing in a random field*, Phys. Rev. B **44** (1991) 12035–12038.

[19] J. Cook and B. Derrida, *Lyapunov exponents of large, sparse random matrices and the problem of directed polymers with complex random weights*, Journal of Statistical Physics **61** (1990) 961–986.

[20] B. Derrida, *Mean field theory of directed polymers in a random medium and beyond*, Physica Scripta **T38** (1991) 6–12.

[21] B. Derrida, M. R. Evans and E. R. Speer, *Mean field theory of directed polymers with random complex weights*, Communications in Mathematical Physics **156** (1993) 221–244.

[22] Y. Y. Goldschmidt and T. Blum, *Directed walks with complex random weights: phase diagram and replica symmetry breaking*, Journal de Physique I **2** (1992) 1607–1619.

[23] B. Derrida, *The zeroes of the partition function of the random energy model*, Physica A: Statistical Mechanics and its Applications **177** (1991) 31–37.

[24] K.J. Wiese and P. Le Doussal, *Functional renormalization for disordered systems: Basic recipes and gourmet dishes*, Markov Processes Relat. Fields **13** (2007) 777–818, cond-mat/**0611346**.

[25] R. Kenyon and A. Okounkov, *Limit shapes and the complex Burgers equation*, Acta Mathematica **199** (2007) 263–302.

[26] S. Kida, *Asymptotic properties of Burgers turbulence*, J. Fluid Mech. **93** (1979) 337.

[27] J. P. Bouchaud and M. Mézard, *Universality classes for extreme-value statistics*, J. Phys. A: Math. Gen. **30** (1997) 7997.

[28] Y. G. Sinai, *Limit behaviour of one-dimensional random walks in random environments*, Teoriya Veroyatnostei i ee Primeneniya **27** (1982) 247–258.

[29] Yu. B. Ovchinnikov, J. H. Müller, M. R. Doery, E. J. D. Vredenbregt, K. Helmerson, S. L. Rolston and W. D. Phillips, *Diffraction of a Released Bose-Einstein Condensate by a Pulsed Standing Light Wave*, Phys. Rev. Lett. **83** (1999) 284–287.

[30] J. Bec and K. Khanin, *Burgers turbulence*, Physics Reports **447** (2007) 1–66.

[31] D. Senouf, *Dynamics and condensation of complex singularities for Burgers' equation I*, SIAM Journal on Mathematical Analysis **28** (1997) 1457.

[32] D. Senouf and R. Caflisch, *Pole dynamics and oscillations for the complex Burgers equation in the small-dispersion limit*, Nonlinearity (1996).

[33] D. Bessis and J. D. Fournier, *Pole condensation and the Riemann surface associated with a shock in Burgers' equation*, Journal de Physique Lettres **45** (1984) 833–841.

[34] D. Bessis, *Complex singularities and the Riemann surface for the Burgers equation*, Research Reports in Physics-Nonlinear Physics, (1990).

[35] E. Medina, M. Kardar and Y. Shapir, *Interference of directed paths in disordered systems*, Phys. Rev. Lett. (1989).

[36] H. Dehling, M. Denker and W. Philipp, *Central limit theorems for mixing sequences of random variables under minimal conditions*, Ann. Prob. (1986) 1359–1370.

[37] R.C. Bradley, *Basic properties of strong mixing conditions. A survey and some open questions*, Probab. Surv. **2** (2005) 107–144.

[38] M. Rosenblatt, *A central limit theorem and a strong mixing condition*, Proceedings of the National Academy of Sciences of the United States of America **42** (1956) 43.

[39] P. Le Doussal, Y. Etzioni and B. Horovitz, *Winding of planar gaussian processes*, Journal of Statistical Mechanics: Theory and Experiment (2009) P07012.

[40] B. Derrida, *Random-energy model: An exactly solvable model of disordered systems*, Phys. Rev. B **24** (1981) 2613–2626.

[41] P. Le Doussal and C. Monthus, *Exact solutions for the statistics of extrema of some random 1d landscapes, application to the equilibrium and the dynamics of the toy model*, Physica A: Statistical Mechanics and its Applications **317** (2003) 140–198.

[42] P. Le Doussal and K.J. Wiese, *How to measure Functional RG fixed-point functions for dynamics and at depinning*, EPL **77** (2007) 66001, cond-mat/**0610525**.

[43] P. Le Doussal, A.A. Middleton and K.J. Wiese, *Statistics of static avalanches in a random pinning landscape*, Phys. Rev. E (2009) **79** (2008) 050101 (R), arXiv:**0803.1142**.

[44] P. Le Doussal and K.J. Wiese, *Size distributions of shocks and static avalanches from the functional renormalization group*, Phys. Rev. E **79** (2009) 051106, arXiv:**0812.1893**.

[45] D. Bernard and K. Gawedzki, *Scaling and exotic regimes in decaying Burgers turbulence*, J. Phys. A: Math. Gen. **31** (1998) 8735.

[46] J. M. Burgers, *The non-linear diffusion equation*, Reidel, Dordrecht, 1974.

[47] A.A. Middleton, P. Le Doussal and K.J. Wiese, *Measuring functional renormalization group fixed-point functions for pinned manifolds*, Phys. Rev. Lett. **98** (2007) 155701, cond-mat/**0606160**.

[48] A. Rosso, P. Le Doussal and K. J. Wiese, *Numerical calculation of the functional renormalization group fixed-point functions at the depinning transition*, Phys. Rev. B **75** (2007).

[49] P. Le Doussal, K. J. Wiese, S. Moulinet and E. Rolley, *Height fluctuations of a contact line: A direct measurement of the renormalized disorder correlator*, Europhys. Lett. **87** (2009) 56001.

[50] L. Balents and P. Le Doussal, *Thermal fluctuations in pinned elastic systems: Field theory of rare events and droplets*, Ann. Phys. **315** (2005) 213–303.

[51] P. Chauve, T. Giamarchi and P. Le Doussal, *Creep and depinning in disordered media*, Phys. Rev. B **62** (2000) 6241–67, cond-mat/**0002299**.

[52] H. Kim and D. A. Huse, *Interfering directed paths and the sign phase transition*, arXiv:**1010.0053**, (2010).

[53] R. Kenyon, A. Okounkov and S. Sheffield, *Dimers and amoebae*, Annals of Mathematics, **163** (2006) 1019–1056.

[54] A. Dobrinevski, P. Le Doussal and K. J. Wiese, unpublished, (2010).

[55] D. Gredat, I. Dornic and J. M. Luck, *On an imaginary exponential functional of Brownian motion*, arXiv:**1101.1173** (2011).